Rev.Adv.Mater.Sci. 18(2008) 565-571

MICROSTRUCTURE AND MAGNETIC PROPERTIES OF Mo CONTAINING NANOPERM-TYPE ALLOYS

C.F. Conde and A. Conde

Departamento de Física de la Materia Condensada, ICMSE-CSIC, Universidad de Sevilla, P.O. Box 1065, 41080 Sevilla, Spain

Received: March 29, 2008

Abstract. The influence of composition changes on the devitrification process, microstructure and magnetic properties of (Fe,Co)MoB(Cu) alloys was investigated. Amorphous and nanocrystalline samples were studied by differential scanning calorimetry, thermomagnetic gravimetry, X-ray diffraction, transmission electron microscopy and vibrating sample magnetometry and obtained results are correlated. Cu addition increases the thermal stability and the crystalline fraction of the nanocrystalline microstructure and improves the soft magnetic properties of the alloy. As B content increases the thermal stability of the nanocrystalline microstructure decreases and for the 20 at.% B alloy boride crystals are formed during the first crystallization stage. Saturation magnetization decreases and Curie temperature of the amorphous phase increases with B content. Co addition lowers the volume fraction of nanocrystals and as Co content increases in the alloy nanocrystals are enriched by Co, Curie temperature of the amorphous phase increases, linearly with Co content, and saturation magnetization and coercive field of nanocrystalline alloys increase as well.

1. INTRODUCTION

Fe-B based nanocrystalline alloys have been extensively explored as highly competitive soft magnetic materials. The origin of the outstanding properties of these alloys is their peculiar two-phase microstructure: ferromagnetic bcc Fe-rich nanosized crystals (~ 10 nm) homogeneously distributed in a residual amorphous phase, also ferromagnetic but with a lower Curie temperature.

Exchange coupling of the crystals, smaller in size than the magnetic interaction length and randomly orientated, via the amorphous matrix provokes that the magnetic anisotropy is reduced. Therefore, soft magnetic properties of these alloys are strongly dependent on the microstructure (size and density of the nanocrystals, i.e. the intergrain distances) and a rapid deterioration of magnetic softness occurs with increasing temperature close to the Curie transition of the residual amorphous phase, which limits the applicability of these materials at high temperatures.

The nanocrystalline microstructure of these materials is usually achieved during primary crystallization of a precursor amorphous alloy when its composition favours a two-stage transformation. Secondary crystallization at higher temperatures produces the complete crystallization of the alloy, destroying the nanocrystalline microstructure, and provokes an abrupt magnetic hardening of the material.

Three main types of soft magnetic nanocrystalline alloys of similar microstructure have been developed: FeSiBNbCu (FINEMET) [1], which show the highest permeability; FeMB(Cu) (M=Zr,Nb,Hf,…) (NANOPERM) [2], with a higher iron content, that exhibit higher saturation magnetization; and FeCoMB(Cu) (HITPERM) [3], with improved high temperature magnetic properties.

Corresponding author: C.F. Conde, e-mail: cfconde@us.es

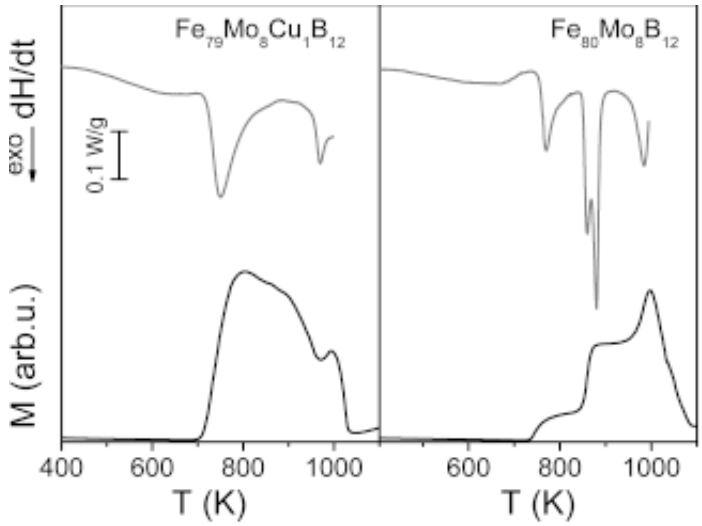

Fig. 1. DSC and TMG plots at 10 K min^{-1} of as-cast samples.

A small Cu addition (1 at.%) was found necessary to develop the nanocrystalline microstructure in FINEMET alloys whereas it can be obtained in Cu-free NANOPERM alloys, although Cu addition refines the grain size. For HITPERM alloys the role of Cu depends on the refractory metal (Zr or Nb) present in the alloy: no microstructural influence of Cu addition was found for $Fe_{44}Co_{44}Zr_7B_4Cu_1$ [4], but a refinement of the grain size was found by Cu containing FeCoNbB alloys with respect to the corresponding Cu free alloys [5].

High attention has been paid to NANOPERM alloys containing Zr or Nb but fewer results can be found dealing with alloys containing other refractory element as Mo [6-10]. Mo alloying provokes a significant decrease of the Curie temperature of the amorphous phase and some compositions, as $Fe_{80}Mo_7B_{12}Cu_1$ [8] are paramagnetic at room temperature. Although this low Curie temperature implies a reduction in the temperature limit for soft magnetic applications of these alloys, amorphous FeMoBCu alloys are being contemplated as candidates for magnetic refrigeration near room temperature [11].

The main aim of this work is to review investigations on the influence of composition changes in the devitrification process, microstructure and magnetic properties of FeMoBCu alloys with a constant 8 at.% Mo content. Effects of Cu addition in $Fe_{80-x}Mo_8B_{12}Cu_x$ (x=0,1) alloys; Fe/B ratio in $Fe_{79-y}Mo_8B_yCu_1$ (y=12,15,17,20) alloys and Co alloying in $(Fe_zCo_1)_{79}Mo_8B_{12}Cu_1$ (z=12,9,6,4,3,2,1) alloys are analyzed.

2. EXPERIMENTAL

Amorphous ribbons 6 mm wide and 20 μm thick were prepared by planar flow casting and compositions were checked by inductionally coupled plasma spectroscopy. Pieces of the as-cast ribbons were heated, at a constant heating rate in Ar atmosphere, up to selected temperatures to obtain different microstructures.

Differential scanning calorimetry (DSC) (Perkin-Elmer DSC 7) and thermomagnetic gravimetry (TMG) (Perkin-Elmer TGA 7) were used to characterize the thermal evolution of the alloys. X-ray diffraction (XRD) (Bruker D8) and transmission electron microscopy (TEM) (Philips CM 200) were used for microstructural characterization. Magnetic properties were measured by vibrating sample magnetometry (VSM) (Lakeshore 7407).

3. RESULTS AND DISCUSSION

3.1. Cu addition in $Fe_{80-x}Mo_8B_{12}Cu_x$ (x=0,1) alloys

Devitrification process appears qualitatively different for Cu containing and Cu free alloys as shown in the DSC plots of Fig. 1. For Cu containing alloy two well resolved exotherms are observed whereas for Cu free alloy the transformation shows a com-

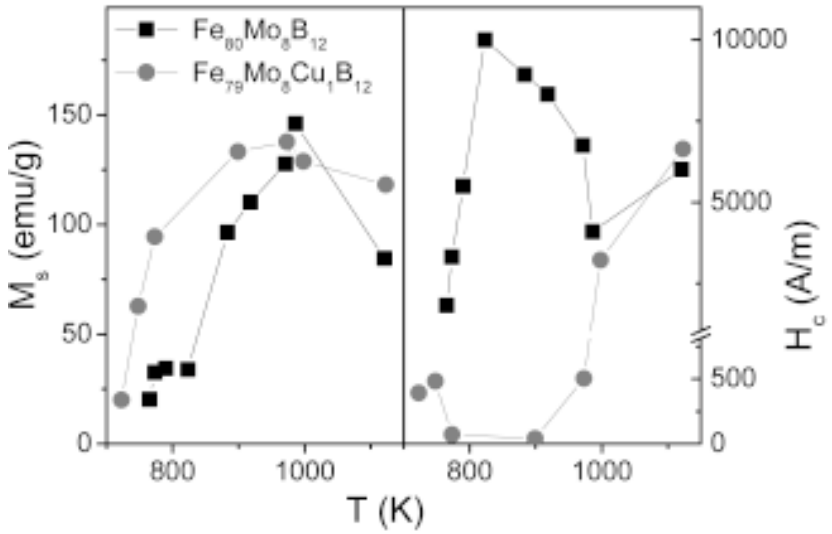

Fig. 2. Room temperature saturation magnetization (left) and coercive field (right) of pre-heated samples.

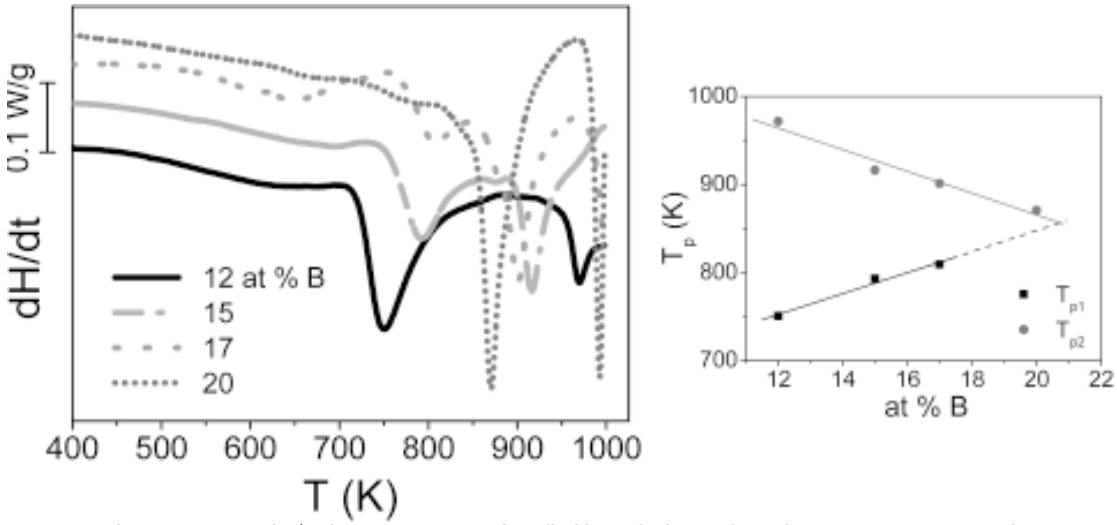

Fig. 3. DSC plots at 10 K min^{-1} of as-cast samples (left) and plots of peak temperatures against B content (right).

plex multi-step process. For both alloys, XRD scans of samples pre-heated up to temperatures around the first DSC exotherm show the lines of a bcc Fe(Mo) phase and the halo of an amorphous phase. TEM images of those samples of both alloys reveal a distribution of nanocrystals in the amorphous matrix, but some microstructural differences between the two alloys can be observed. For Cu containing alloy nanocrystals, 7-9 nm in diameter, appear homogeneously dispersed in the amorphous matrix whereas for Cu free alloy bigger nanocrystals appear inhomogeneously dispersed in the matrix and show a broader grain size distribution. For the Cu free alloy, after the second and third overlapped exotherms, XRD scan shows the lines of a bcc Fe(Mo) phase together others lines of an unidentified phase but the amorphous halo is still present. Secondary crystallization, occurring above 900K for both alloys, is a rather complex process after which samples are fully crystalline. The formation of boride phases includes recrystallization processes involving some of the primary Fe-rich crystals, as found for FeCoNbB alloys [12].

Low-field (~ 20 mT) magnetization plots of both alloys (Fig. 1) show a paramagnetic behaviour below the crystallization onset and subsequent increase in magnetization, associated to the forma-

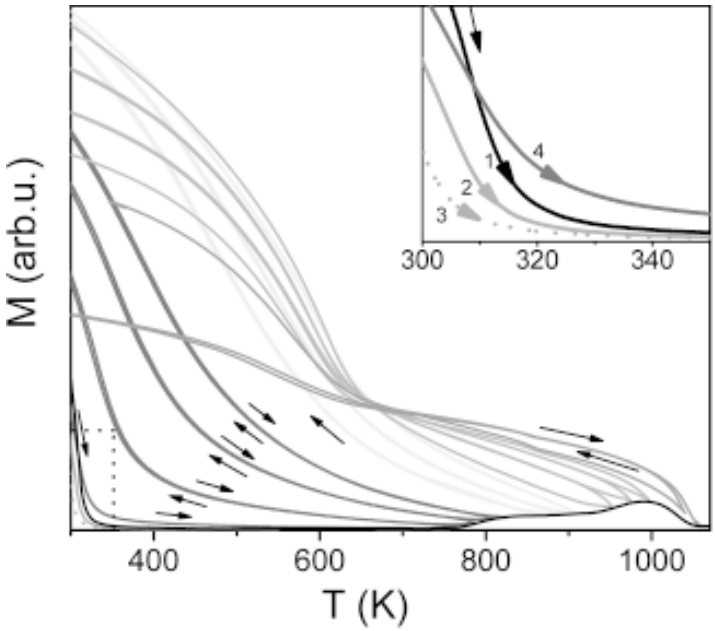

Fig. 4. Low-field magnetization plots showing the effects on the Curie temperatures of successive heating-cooling cycles up to a higher temperature each cycle. Marked area is enlarged in the inset to show the decrease of *Tc* during relaxation. Successive heatings are indicated by numbers.

tion of ferromagnetic phases at the different crystallization steps, at temperatures in good agreement with the DSC exotherms. Magnetization curves reveal some differences in the secondary crystallization of the two alloys. Finally, at higher temperature, magnetization falls due to the Curie transition of ferromagnetic phases previously formed.

Fig. 2 shows room temperature saturation magnetization and coercive field of samples pre-heated up to different temperatures, obtained from hysteresis loops taken at the VSM with a maximum applied field of 5 kOe. For Cu containing alloy saturation magnetization increases with the volume fraction of bcc Fe-(Mo) crystals and decreases at the second crystallization stage. Coercive field slightly increases at the beginning of the primary crystallization, probably due to an insufficient exchange coupling of the grains, and decreases for higher crystalline fractions as the decreasing in intergranular distances results in a stronger coupling of the crystals. At the second crystallization stage an abrupt increase in coercivity is observed, associated to the formation of boride phases. For Cu free alloy saturation magnetization shows smaller values than for the Cu containing alloy. Coercive field abruptly increases at the appearance of the unidentified phase during second exotherm, to decrease at higher temperature, probably due to a coarsening in grain size, and a magnetic hardening is observed at the secondary crystallization stage.

3.2. Different Fe/B ratio in $Fe_{79-y}Mo_8B_yCu_1$ (y=12,15,17,20) alloys

Devitrification of these alloys (Fig. 3) is a complex multi-step transformation [9]. A linear dependence of the peak temperatures, T_{p1} and T_{p2}, of the two major exotherms with the alloy B content is found: T_{p1} increases and T_{p2} decreases as the B content increases and the two fitting lines intersect at 20 at.% B content (Fig. 3).

For samples of this alloy pre-heated up to the end of the first exotherm XRD and TEM reveal the presence of boride crystals along with bcc Fe-(Mo) crystals and amorphous phase. The volume fraction of bcc-Fe(Mo) crystals is drastically reduced

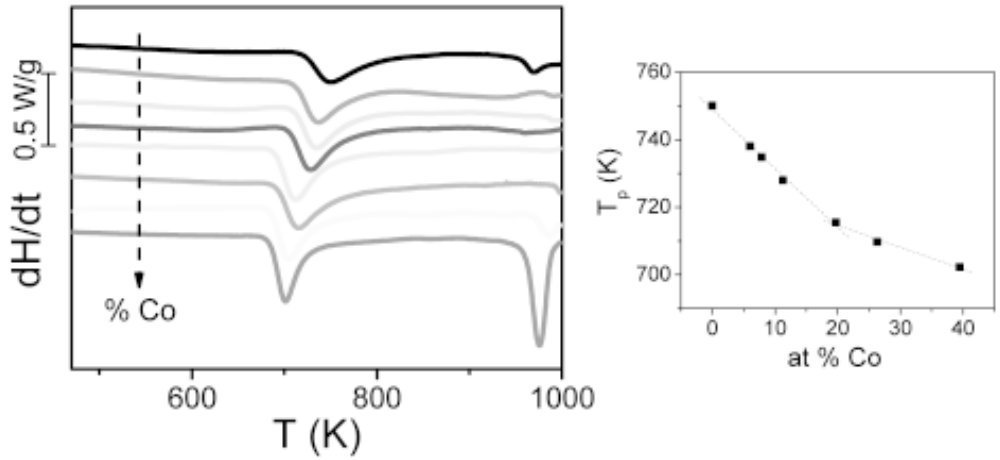

Fig. 5. DSC plots at 10 K min^{-1} of as-cast samples (left) and a plot of the peak temperature against Co content (right).

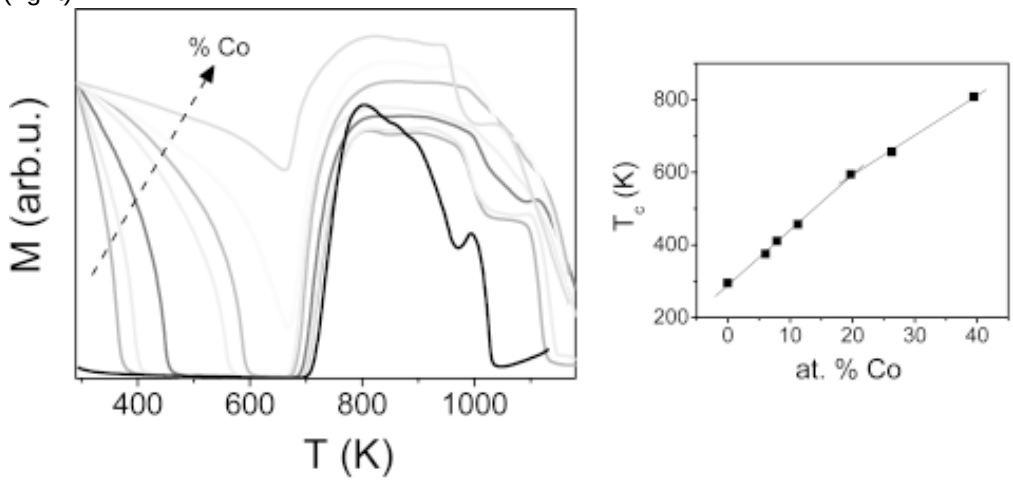

Fig. 6. TMG plots at 10 K min^{-1} of as-cast samples (left) and a plot of Curie temperature of amorphous against Co content.

in this alloy in relation to that of the lower B content alloys.

Curie temperature of as-cast amorphous samples increases linearly (~ 10 K/at.% B) with the B content in the alloy. Extrapolation of the fitting line to low B content values agrees with the observed paramagnetic state of the 12 at.% B alloy at room temperature. Low field magnetization shows the usual thermal evolution found for these alloys.

Annealing effects on the Curie temperature can be observed in Fig. 4 for the 15 at.% B alloy. A similar behaviour is found in all the studied alloys. An initially amorphous sample was submitted to successive heating-cooling cycles from room temperature up to a temperature, about 25K higher each time, inside the range 650-1100K. Inset in Fig. 4 is an enlargement of the marked area in the figure showing part of the heating curve of the four first cycles. Relaxation in amorphous samples decreases the Curie temperature (plots 1-3 in the inset), as previously found for analogous alloys [9,10]. For nanocrystalline samples the Curie temperature of the residual amorphous phase increases with the crystalline fraction becoming less defined. Magnetization decreases after the secondary crystallization stage and shows the existence of, at least, two magnetic phases in fully crystalline samples.

For each composition room temperature saturation magnetization of pre-heated samples increases with the crystalline fraction but, for each pre-heating temperature, magnetization decreases

as the B content in the alloy increases. Coercive field of pre-heated samples shows the above described dependence with microstructural evolution. For all the compositions the lowest coercivity corresponds to the end of the nanocrystallization process and the softest material is found to be the 17 at.% B alloy [13].

3.3. Co substitution in $(Fe_zCo_1)_{79}Mo_8B_{12}Cu_1$ (z =12,9,6,4,3,2,1) alloys

Devitrification process of these (FeCo)MoBCu alloys (Fig. 5) consists of at least two stages, the second of them above 950K. The crystallization onset decreases as the Co content in the alloy increases. An almost linear dependence of the peak temperature with the Co content of the alloy is found although a change in slope at 20 at.% Co can be observed in the plot of Fig. 5. X-ray scans of samples pre-heated up to the end of the first DSC exotherm show the lines of a α-Fe(Co,Mo) phase and a broad halo revealing the residual amorphous phase. Lattice parameter of the α-Fe(Co,Mo) phase decreases as the Co content in the alloy increases, indicating an increase of Co content of the crystalline grains as the alloy in enriched by Co.

The crystalline fraction at the end of primary crystallization decreases from ~ 65% for Co free alloy to ~ 55% for all the Co studied alloys. TEM images show a slight decrease in grain size of primary crystals as the Co content increases in the alloy [14].

Thermal dependence of low-field magnetization (Fig. 6) shows the behaviour above described but, as Co content in the alloy increases, the combined effect of the increase in the Curie temperature and the decrease of the crystallization onset provokes that the fall in magnetization at Curie transition overlaps with its increase at the primary crystallization. Saturation magnetization increases with the Co content in the alloy for amorphous and nanocrystalline samples and coercive field of nanocrystalline samples also increases with the Co content in the alloy.

4. CONCLUSIONS

From the described results on (FeCo)MoB(Cu) alloys we can conclude:

(i) Cu is not needed to develop a nanocrystalline microstructure in these alloys but its thermal stability is significantly reduced and the volume fraction of nanocrystals is lower in Cu free alloys. Cu addition improves the soft magnetic properties of the alloy.

(ii) The thermal stability of the nanocrystalline microstructure decreases as the alloy B content increases and for the 20 at.% B alloy boride crystals are formed during the first crystallization stage. Saturation magnetization decreases and Curie temperature of the amorphous phase increases with B content. The softest magnetic material is the 17 at.% B nanocrystalline alloy.

(iii) Co addition lowers the volume fraction of nanocrystals and the grain size is slightly reduced with Co content in the alloy. Nanocrystals are enriched by Co as Co content in the alloy increases. Curie temperature of the amorphous phase increases linearly with Co content. Saturation magnetization and coercive field of nanocrystalline alloys increases with Co alloying.

ACKNOWLEDGEMENTS

Work supported by the Spanish Government and EU FEDER (Project MAT 2004-04618) and the PAI of the Junta de Andalucía.

References

[1] Y. Yoshizawa, S. Oguma and K.Yamauchi // *J. Appl. Phys.* **64** (1988) 6044.

[2] K. Suzuki, A. Makino, N. Kataoka, A. Inoue and T. Masumoto // *Mater.Trans. JIM* **32** (1991) 93.

[3] M.A. Willard, D.E. Laughlin, M.E. McHenry, D. Thoma, K. Sickafus, J.O. Cross and V.G. Harris // *J. Appl. Phys.* **84** (1998) 6773.

[4] D.H. Ping, Y.Q. Wu, K. Hono, M.A. Willard, M.E. McHenry and D.E. Laughlin // *Scripta Mater.* **45** (2001) 781.

[5] J.S. Blázquez, V. Franco and A. Conde // *J. Phys.: Condens. Matter* **14** (2002) 11717.

[6] B. Idzikowski, J. Baszynski, I. Skorvanek, K.H. Müller and D. Eckert // *J. Magn. Magn. Mater.* **177-181** (1998) 941.

[7] M. Miglerini, M. Kopcewicz, B. Idzikowski, Z.E. Horvath, A. Grabias, I. Skorvanek, P. Duzewski and C.S. Daroczi // *J. Appl. Phys.* **85** (1999) 1014.

[8] M. Müller, H. Grahl, N. Mattern and B. Schnell // *Mater. Sci. Eng. A* **304-306** (2001) 353.

[9] E. Illekova, D. Janickovic, M. Miglerini, I. Skorvanek and P. Svec // *J. Magn. Magn. Mater.* **304** (2006) e636.

[10] C.F. Conde, A. Conde, D. Janickovic and P. Svec // *J. Magn. Magn. Mater.* **304** (2006) e739.
[11] V. Franco, C.F. Conde, J.S. Blázquez, A. Conde, P. Svec and D. Janickovic, to be published.
[12] J.S. Blázquez, C.F. Conde and A. Conde // *Appl. Phys. Lett.* **79** (2001) 2898.
[13] C.F. Conde, J.S. Blázquez, V. Franco, A. Conde, D. Janickovic and P. Svec, to be published.
[14] C.F. Conde, J.M. Borrego, J.S. Blázquez, A. Conde, D. Janickovic and P. Svec, to be published.